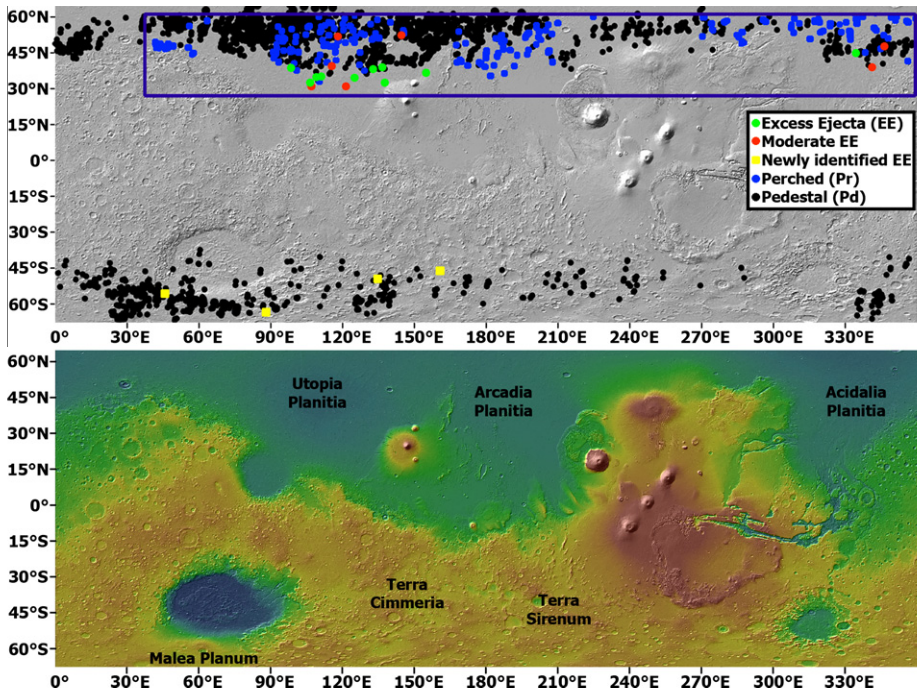

Fig. 10. The top map shows the geographic distribution of excess ejecta craters (green dots) and moderately excess ejecta craters (red dots) from Black and Stewart (2008), perched craters (blue dots) from Boyce et al. (2005), pedestal craters (black dots) from Kadish et al. (2009), and newly identified excess ejecta craters in the southern hemisphere (yellow squares). The bottom map, which shows MOLA topography, identifies significant regions of interest. Due to the limited geographic extent of previous surveys for EE and Pr, we have outlined the general region over which they were identified with a purple box. Note, however, that neither the EE nor the Pr survey included the entire area of the purple box; the EE survey covered only 86–163°E and 308–355°E for the latitudes shown (Black and Stewart, 2008), while the Pr survey was limited to distinct rectangular regions based on the available MOLA 1/128° DEM (Boyce et al., 2005). In addition, both the EE and Pr studies ignored craters smaller than 4 and 6 km in diameter, respectively. Despite these limitations, the distribution shows clear similarities in where EE, Pr, and Pd form, with the highest concentrations in Utopia and Acidalia Planitia, and the new southern hemisphere EE are all located in regions where Pd are present. In terms of population density, these data show that Pd are the most widespread, while EE are the least common. (For interpretation of the references to colour in this figure legend, the reader is referred to the web version of this article.).

similar profiles. We then detrended the profiles by subtracting the regional topographic slopes, which we derived from profiles of the plains surrounding the craters to a distance of at least 15 km beyond the extent of the ejecta deposits. These linear slopes were interpolated over the crater basin to establish the elevation of the pre-impact surface at the point of impact. Averaging these profiles for each individual crater allowed us to measure the crater depth and width and the average excess ejecta thickness. Crater depths were confirmed using MOLA shot data. It should be reiterated that, in this case, crater depth refers to the difference in elevation between the surrounding plains and the deepest point of the crater basin, and is not dependent on the crater rim height. We then measured the areal extent of the ejecta and multiplied this by the average excess ejecta thickness to get the excess ejecta volume (V_{ejecta}). To calculate the crater volume (V_{cavity}), we ran a best-fit algorithm on the averaged crater profiles, allowing it to select from a hyperbolic, conic, or parabolic (power law) equation. In each case, the best-fit was a parabola with a correlation coefficient of >0.98. The resulting equation was then rotated around the z-axis to create a paraboloid, and integrated according to the depth of the crater. We also tested HRSC DTM profiles and gridded MOLA profiles separately to ensure that differences in dataset resolution had no bearing on our results. The HRSC and MOLA profiles always yielded volumetric measurements within 2% of each other; this degree of error is trivial in determining whether the examined fresh craters qualify as excess ejecta craters. Using these values, we were able to confirm the presence of four craters with V_{cavity}/V_{ejecta} greater than 2.5 (Fig. 11 and Table 2). It should be noted that, by using the techniques set forth by Black and Stewart (2008), we assume that the typical V_{cavity}/V_{ejecta} is not significantly different for craters in the southern hemisphere, and thus a value of 2.5 is still 3σ from the average.

Interestingly, no EE were identified that had a diameter greater than 3 km (Table 2). Because Black and Stewart (2008) only measured fresh craters larger than 4 km, these new EE are considerably smaller than those previously analyzed. There is, however, one EE of comparable size, named Vaduz, which has been analyzed in detail by Schaefer et al. (2011). Because these craters are so small, they are readily susceptible to erosion. As such, the rarity of their presence, having survived the sublimation and removal of the surrounding ice-rich target layer, is not surprising. The new EE, in addition to having small diameters, also have relatively thin excess ejecta (16–26 m) compared to measurements by Black and Stewart (2008). The ejecta of these EE examples is always of the DLE type and is remarkably extensive compared to the sizes of the craters (Fig. 11). The small volumes of the crater cavities and large extents of their ejecta yield high V_{cavity}/V_{ejecta} values, reaching up to 28.5 (Table 2). Unlike the northern hemisphere examples, these EE appear to have relatively smooth ejecta, although this interpretation may be hindered by limitations of the image resolution; some portions of the ejecta do appear rougher than others, and there are signs of sublimation pits on the surface of at least one of the new EE ejecta deposits (Fig. 11A).

The newly identified EE are located exclusively between 45°S and 65°S, and are all in the eastern hemisphere, which is where the vast majority of southern hemisphere Pd are located (Fig. 10). These EE are not, however, within close proximity of each other. Each is located in or near a Pd field (within hundreds of km), and we have identified one example that is only tens of km from two Pr (Fig. 11b). This distribution is consistent with the findings of the northern hemisphere geographic distribution, as discussed in the previous section; each of the three morphologies tends to occur and be concentrated in the same regions, and multiple morphologies are often seen within the same image (Figs. 2 and 5).